Research Article Open Access

Mária Minárová\* and Jozef Sumec

# Stress - Strain Response of the Human Spine Intervertebral Disc As an Anisotropic Body. Mathematical Modeling and Computation.

DOI 10.1515/phys-2016-0047 Received June 8, 2016; accepted October 17, 2016

**Abstract:** The paper deals with the biomechanical investigation on the human lumbar intervertebral disc under the static load. The disc is regarded as a two - phased ambient consisting of a fibrous outer part called annulus fibrosis and a liquid inner part nucleus pulposus. Due to the fibrous structure, the annulus fibrosis can be treated by using a special case of anisotropy - transversal isotropy.

In the paper the corresponding tensor of material constants is derived. The tensor consequently incomes to the constitutive equations determining the stress - strain relation in the material. In order to study the mechanical behaviour the disc is observed within the motion segment, the basic unit for motion tracing. The motion segment involves two neighbouring vertebrae and the intervertebral disc between them that connect them both.

When constitutive equations are accomplished, they can be incorporated in the finite element analysis. The illustrative example of the intervertebral disc L2/L3, the disc between the second and the third lumbar vertebrae the lumbar part of spine, with its computer implementation is performed. Finally the comparison of the results of using anisotropic and homogenized approach is provided. The comparison illustrates the eligibility of such a kind of approach.

**Keywords:** annulus fibrosis, anisotropic material tensor, constitutive equation

PACS: 87.85.gp, 02.10.Ud

Jozef Sumec: Dpt. of Structural Mechanics, Faculty of Civil Engineering, Slovak University of Technology, Bratislava 81005, Slovak Republic, E-mail: jozef.sumec@stuba.sk

# 1 Introduction

Nowadays, the lower back pain has become the civilisation disease. The causes of such a problem are diverse the long-lasting sitting at work, overloading of the back by persisting repeating load, predisposition caused by previous diseases, bad nourishment, stress, insufficiency or absence of sport activities, injury etc. The most people suffering of the low back pain are treated by non-invasive methods as the physiotherapy, rehabilitation, by medicaments, by using orthopaedic supporting mechanism, etc. In worse cases when the progress of the disease is irreversible, the invasive methods, the surgery intervention is inevitable. Hence, the previous theoretical investigations, analyses, predeterminations foregoing the operation are welcome. The artificial replacements' mechanical behaviour are observed, computed and tested within the biomechanics. Of course, the biocompatibility has to be regarded. The biocompatibility of materials with human tissue, the stimulation of tissue growth by therapeutic cells seeding into the degenerative disc, scaffolds methods, this is the task of the new interdisciplinary branch of research called tissue engineering, see e.g. [1]. The predicting or tracing of the tissue growth can be carried out by using the fractal analysis as well, see e.g. [7].

The expansion of the mathematical and computational modelling in recent decades facilitated the biomechanical research inter alia, enabled to simulate, observe and predict some processes of living organisms. A term "virtual human reality" is recently used, that involves the wide spectrum of biomechanical investigation of the systems and processes within the human body, [3].

In 1974 Belytschko et al. [2], created the first onedimensional axisymmetric mechanical model of the intervertebral disc (ID) loaded uniformly. Afterwards, in 1976, Kulak et al. [9], incorporated the non linear material properties of the annulus fibrosis (AF) into the existing model. Since the vertebrae shape and dimensions varies from person to person, there was a need to generalize the morphology of the particular vertebrae alongside the spine. Spilker

<sup>\*</sup>Corresponding Author: Mária Minárová: Dpt. of Mathematics and Descriptive Geometry, Faculty of Civil Engineering, Slovak University of Technology, Bratislava 81005, Slovak Republic, E-mail: maria.minarova@stuba.sk

did so in 1982 in [15] and this paper provides the general dimensions of particular vertebrae. At the same time he points out to the dimensions which are decisive in mechanical responses tracing.

The generalized dimensions are obviously taken as an input of the investigation. In our paper that deals with physical equations for annulus fibrosis - the collagen external part of the ID, we also took the dimensions from [15].

# 2 Motivation

The anatomical observing of a human intervertebral disc reveals that the outer part of a human intervertebral disc the annulus fibrosis consists of 10-12 lamellae formed from an inherent amorphous matter, each of them being encapsulated by the spiral system of parallel fibres. The slope of ascending of the spiral system is  $tg(\pm \alpha)$ , the sign switching from lamella to lamella. Alternating sign in front of  $\alpha$ means the neighbouring lamellae have always the fibres ascendancy in reverse direction. The angle of crossing the neighbouring lamellae fibres varies from 48° up to 74°. The thickness of the fibre is  $1 - 5\mu m$ . The distance between fibres is almost the same as the distance between the lamellae. In radial direction the number of the fibres is variable, the density is evenly ordered along the circumference. The collagen fibres are not interconnected with the body of the vertebra. More details concerning intervertebral disc anatomy can be found e.g in [13]. For the sake of further biological and numerical handling of the stress vs. strain ( $\sigma \sim \varepsilon$ ) relation within the anisotropic model of intervertebral disc it is required to switch between the local coordinate system (LCS) and global coordinate system (GCS). Herein LCS arises naturally from the configuration of the fibres with-inside the annulus fibrosis and the GCS following the accordance with the entire spine geometry. Herein, the local coordinate system utilizes the quasi cyclic symmetry due to sheeted topology of the curved collagen fibres systems. Both forward and backward switchover between LCS and GCS is realized by the transformation matrices. All mathematical points, covering geometry and physical properties, tided with switching between LCS and GCS are treated in this paper. Such a treatment farther enables us to deal with anisotropy conveniently. This mathematical investigation is the main contribution of the paper.

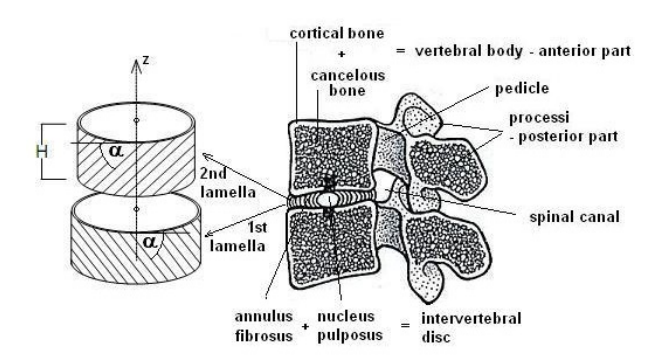


Figure 1: Right: Spinal motion unit section; left: collagen fibres arrangement structure within the intervertebral disc annulus

# 3 Mathematical modelling

For the proper mathematical investigation we impose some basic biological, mathematical and physical assumptions.

# 3.1 Assumptions

- the analysed body (intervertebral disc) is supposed to be a continuum
- investigations are done within the linear elasticity theory
- the fibres of annulus fibrosis are of the homogeneous material; its physical properties are subjected to the generalized Hook law; the nucleus of the ID is a viscous medium
- inner initial stresses and thermal influences are negligible
- quasi static external load is assumed
- deterministic phenomenological mathematical model is concerned

# 3.2 Lagrange variational principle application

It is well known fact that Lagrange variational principle comes from virtual displacement principle, see e.g. [17]. This can be written as

$$\int_{V} (\sigma_{ij} \delta \varepsilon_{ij} - \hat{X}_{i} \delta u_{i}) dV - \int_{S_{P}} \hat{p}_{i} \delta u_{i} dS = 0; \quad (i, j = x, y, z)$$
(3.1)

with  $\sigma_{ij}$  being stress Cauchy tensor components,  $\varepsilon_{ij}$  small deformation Green tensor components,  $\delta u_i$  point displacement vector variation components,  $\hat{p}_i$ ,  $\hat{X}_i$  prescribed sur-

face and volume forces vectors, V volume of the domain  $\Omega$  (intervertebral disc),  $S_P$  boundary of the domain  $\Omega$  - the surface where the surface forces are prescribed. Here and further the given values - known ones - are these ones with the hat above. The deformation potential energy density  $W(\varepsilon_{ij})$  reads

$$\sigma_{ij} = \frac{\partial \mathcal{W}}{\partial \varepsilon_{ij}} \tag{3.2}$$

in each component. Substituting (3.2) to (3.1) then yields

$$\int_{V} \frac{\partial W}{\partial \varepsilon_{ij}} \delta \varepsilon_{ij} dV - \int_{V} \hat{X}_{i} \delta u_{i} dV - \int_{S_{n}} \hat{p}_{i} \delta u_{i} dS = 0$$
 (3.3)

The first term in (3.3) represents the first variation of the deformation potential energy,  $\delta \mathcal{U}$ . Having the fixed volume and surface forces  $\hat{X}_i$  and  $\hat{p}_i$ , the last two integrals in (3.3) can be merged in the variation of external forces potential energy  $\delta \mathcal{L}$ . Accordingly, the virtual displacement principle is given by the known relation

$$\delta \mathcal{U} + \delta \mathcal{L} = \delta (\mathcal{U} + \mathcal{L}) = \delta \Pi = 0 \tag{3.4}$$

The quadratic functional (3.4) acquires its minimum on the set of admissible variations of the real displacements, e.g. [11].

# 3.3 Constitutive equations of the intervertebral disc

Due to layered lamellae structure of ID known from the anatomy, due to the physical properties of the collagen fibres and due to their spiral configuration, the intervertebral disc is modelled as a transversally isotropic composite ambient.

Let us define a local Cartesian coordinate system, an ordered triple  $(x_1, x_2, x_3) = (1, 2, 3)$  where the axis  $x_1 \equiv 1$  is parallel to the fibres direction, the axis  $x_2 \equiv 2$  is perpendicular to the fibres direction, lying on the tangent plane to the lamella and the axis  $x_3 \equiv 3$  is perpendicular to the  $(x_1, x_2)$  plane. Let us suppose the global coordinate system  $(r, t, z) = (\bar{1}, \bar{2}, \bar{3})$  which is rotated from the local coordinate system by the angle  $\alpha$ , with  $x_3 = 3$  being the axis of rotation, see Fig. 2. While forming the constitutive, i.e. physical equations for the transversally isotropic material we start from the generalized Hook law for anisotropic body. The Cauchy stress tensor  $\sigma_{ij}$  is of the form

$$\sigma_{ij} = c_{ijkl} \varepsilon_{kl} \tag{3.5}$$

with  $c_{ijkl}$  being the elastic coefficients united in the elastic tensor operator with 81 coefficients and  $\varepsilon_{kl}$  the Green deformation tensor components. By using the symmetry of

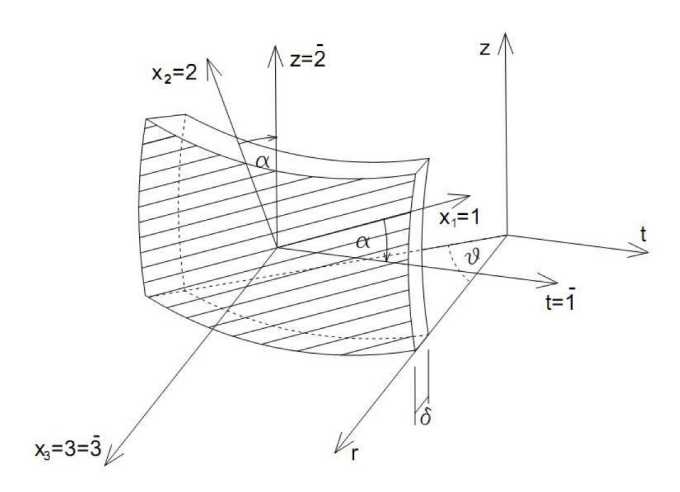


**Figure 2:** Intervertebral disc lamella fragment with the "old" local  $(x_1, x_2, x_3) = (1, 2, 3)$  and "new" (r, t, z) coordinate system with  $\alpha$  being the slope of the fibre ascending

the stress tensor  $\sigma_{ij} = \sigma_{ji}$ , (i, j = 1, 2, 3) and the symmetry of the strain tensor  $\varepsilon_{kl} = \varepsilon_{lk}$ , (k, l = 1, 2, 3) the number of coefficients decreases to 36. Moreover, subject to thermodynamic laws, it is possible to prove, the validity of the relation, [5]

$$c_{ijkl} = c_{klij} \tag{3.6}$$

$$s_{ijkl} = s_{klij} \tag{3.7}$$

(3.6) performs the double symmetry of the compliance and (3.7) matrix coefficients. In the most general case the terms (3.6) decrease the number of the coefficients to 21. Due to the 2nd law of thermodynamics it can be shown that the tensor operators  $c_{ijkl} = (s_{ijkl})^{-1}$  is a positive definite operator [11]. Relation (3.5) can be then rewritten in the reverse form

$$\varepsilon_{ij} = s_{ijkl}\sigma_{kl}, \quad (i, j = 1, 2, 3)$$
 (3.8)

Note 1:

a) If an elastic theory problem is elaborated on the atomic level, by using some other assumptions, the number of the coefficient can be even more decreased. This depends on the crystal character and composition of the material [5]. b) Since we have restricted our investigation to the Cartesian coordinate system, we need not to distinguish between covariant and contra-variant tensors. Moreover, as we would like to make the notation more simple, we establish the restriction of the indexes number of stress  $\sigma_{ij}$  and

strain  $\varepsilon_{ii}$  in the following way:

$$11 \rightarrow 1,22 \rightarrow 2,33 \rightarrow 3,12 \rightarrow 4,23 \rightarrow 5,31 \rightarrow 6 \ \ \mbox{(3.9)}$$

$$\sigma_{ij} = \begin{cases}
\sigma_{11}, \ \sigma_{22}, \ \sigma_{33}; & \sigma_{12}, \ \sigma_{23}, \ \sigma_{31} \\
\sigma_{1}, \ \sigma_{2}, \ \sigma_{3}; & \sigma_{4}, \ \sigma_{5}, \ \sigma_{6}
\end{cases} (3.10)$$

$$\varepsilon_{ij} = \begin{cases}
\varepsilon_{11}, \ \varepsilon_{22}, \ \varepsilon_{33}; & 2\varepsilon_{12}, \ 2\varepsilon_{23}, \ 2\varepsilon_{31} \\
\varepsilon_{1}, \ \varepsilon_{2}, \ \varepsilon_{3}; & \varepsilon_{4}, \ \varepsilon_{5}, \ \varepsilon_{6}
\end{cases} (3.11)$$

$$\varepsilon_{ij} = \begin{cases} \varepsilon_{11}, \ \varepsilon_{22}, \ \varepsilon_{33}; & 2\varepsilon_{12}, \ 2\varepsilon_{23}, \ 2\varepsilon_{31} \\ \varepsilon_{1}, \ \varepsilon_{2}, \ \varepsilon_{3}; & \varepsilon_{4}, \ \varepsilon_{5}, \ \varepsilon_{6} \end{cases}$$
(3.11)

This restriction of the indexes decreases the order of the tensor twice. In the such a way e.g. a matrix will be aligned to a vector, a tensor of the 4th order will acquire the form of matrix. Hence, we will reduce the number of indexes twice. In the following text we will use  $\sigma_5$  instead of  $\sigma_{23}$ ,  $\varepsilon_3$  instead of  $\varepsilon_{33}$ ,  $\varepsilon_4$  instead of  $2\varepsilon_{31}$ . Moreover using the index restriction (3.9) also for tensors  $c_{iikl}$  and  $s_{iikl}$ , we will write  $c_{11}$  instead of  $c_{1111}$ ,  $s_{36}$  instead of  $s_{3331}$ ,  $c_{15} = c_{51}$  instead of  $c_{1123} = c_{2311}$ ,  $s_{26} = s_{62}$  instead of  $s_{2231} = s_{3122}$ , etc. Hereinafter we utilize the differentiability of the elastic deformation energy density function W. Its differential when using the Einstein summation convention and considering the Note 1 can be expressed in the form

$$dW = \sigma_i d\varepsilon_i = c_{ii} \varepsilon_i d\varepsilon_i \tag{3.12}$$

i.e., for entire body of the volume V

$$W = \int_{V} dW(\varepsilon_i) = \int_{V} c_{ij} \varepsilon_j d\varepsilon_i$$
 (3.13)

I accordance with Assumptions in Chapter III.A, the domain  $\Omega$ , i.e. intervertebral disc is considered as fully elastic, which ensures the linearity herein and integral in (3.13) does not depend on the integration path. Here, the necessary and sufficient condition is dW being the total differential of function  $W(\varepsilon_i)$ , i.e.

$$dW = \frac{\partial W}{\partial \varepsilon_i} d\varepsilon_i \tag{3.14}$$

By comparing the equations (3.12) and (3.14) we get

$$\frac{\partial \mathcal{W}}{\partial \varepsilon_i} = c_{ij}\varepsilon_j \tag{3.15}$$

Exploitating the fact that  $W = W(\varepsilon_i)$  is a differentiable function we can write

$$\frac{\partial^2 \mathcal{W}}{\partial \varepsilon_i \partial \varepsilon_j} = c_{ij} \tag{3.16}$$

respectively

$$\frac{\partial^2 \mathcal{W}}{\partial \varepsilon_i \partial \varepsilon_i} = c_{ji} \tag{3.17}$$

The fact, that the order which the derivatives are performed is not dependent on the structure of the material,

the symmetry of the elastic coefficients (mathematically) implies

$$c_{ii} = c_{ii} \tag{3.18}$$

That is why the matrix of elastic constants has 21 elements. Hence, the equation (3.13) in the unit volume can be rewritten as

$$W = \frac{1}{2}c_{ij}\varepsilon_i\varepsilon_j, \quad (i, j = 1, ..., 6)$$
 (3.19)

Similarly, the validity of the relationship

$$W = \frac{1}{2} s_{ij} \sigma_i \sigma_j, \quad (i, j = 1, ..., 6)$$
 (3.20)

can be proved, e.g. [10], whereas  $s_{ii}$  are the elastic moduli components that read

$$s_{ij} = [c_{ij}]^{-1}, \quad (i, j = 1, ..., 6)$$
 (3.21)

Let us suppose in each point of  $\Omega$  there exists a plane of symmetry, e.g. (1,2) - tangent plane to the lamella of the intervertebral disc, see Fig. 2). Then

$$c_{ii} = 0, \quad (i = 1, 2, 3 \land j = 5, 6)$$
 (3.22)

In this way the number of coefficients decreases to 13. In each point of the domain  $\Omega$  there exist three planes of symmetry, planes (1,2), (2,3), (3,1), perpendicular each other. That implies  $\Omega$  is an orthotropic body that in addition reads

$$c_{ii} = 0$$
,  $(i = 1, 2, 3, 5 \land i = 4, 6)$  (3.23)

Due to the elastic symmetry  $c_{ij} = c_{ji}$  the number of elastic coefficient decreases to 9. Finally, the corresponding compliance matrix, i.e the matrix involving the elastic moduli coefficients, is

$$\mathbf{S} = [s_{ij}] = \begin{bmatrix} \frac{1}{E_1} & -\frac{v_{21}}{E_2} & -\frac{v_{31}}{E_3} & 0 & 0 & 0\\ -\frac{v_{12}}{E_1} & \frac{1}{E_2} & -\frac{v_{32}}{E_3} & 0 & 0 & 0\\ -\frac{v_{13}}{E_1} & -\frac{v_{23}}{E_2} & \frac{1}{E_3} & 0 & 0 & 0\\ 0 & 0 & 0 & \frac{1}{G_{12}} & 0 & 0\\ 0 & 0 & 0 & 0 & \frac{1}{G_{23}} & 0\\ 0 & 0 & 0 & 0 & 0 & \frac{1}{G_{23}} \end{bmatrix}$$
(3.24)

with  $\frac{v_{ij}}{E_i} = \frac{v_{ji}}{E_i}$ , (i, j = 1, 2, 3). In matrix (3.24) the material constants  $E_1, E_2, E_3$  are the directional elastic moduli in the 1,2 and 3 axes direction, see Fig. 2;  $v_{ij}$  are Poisson coefficients of the transversal deformation with  $v_{ij} = -\varepsilon_i/\varepsilon_i$  and  $G_{12}$ ,  $G_{23}$ ,  $G_{31}$  are the shear moduli corresponding to the planes (1,2), (2,3), (3,1). Thus, the orthotropic body reads

$$\sigma_{1} = c_{11}\varepsilon_{1} + c_{12}\varepsilon_{2} + c_{13}\varepsilon_{3} 
\sigma_{2} = c_{21}\varepsilon_{1} + c_{22}\varepsilon_{2} + c_{23}\varepsilon_{3} 
\sigma_{3} = c_{31}\varepsilon_{1} + c_{32}\varepsilon_{2} + c_{33}\varepsilon_{3} 
\sigma_{4} = c_{44}\varepsilon_{4}; \sigma_{5} = c_{55}\varepsilon_{5}; \sigma_{6} = c_{66}\varepsilon_{6}$$
(3.25)

The deformation energy density (3.19) can be rewritten in details  $\mathcal{W} = \frac{1}{2}c_{11}\varepsilon_1^2 + c_{12}\varepsilon_1\varepsilon_2 + c_{13}\varepsilon_1\varepsilon_3 + \frac{1}{2}c_{22}\varepsilon_2^2 + c_{23}\varepsilon_2\varepsilon_3 + \frac{1}{2}c_{33}\varepsilon_3^2 + \frac{1}{2}c_{44}\varepsilon_4^2 + \frac{1}{2}c_{55}\varepsilon_5^2 + \frac{1}{2}c_{66}\varepsilon_6^2$ . In our case, regarding to the structure of the intervertebral disc annulus its layered configuration of lamellae and twisted collagen fibres, we will suppose that the plane (2,3) is the isotropy plane, which means the constants  $c_{ii}$  will read

$$c_{12} = c_{13}, c_{22} = c_{33}, c_{44} = c_{66}$$
 (3.26)

So, it remains 9 - 3 = 6 different material constants  $c_{11}$ ,  $c_{12}$ ,  $c_{22}$ ,  $c_{23}$ ,  $c_{44}$ ,  $c_{55}$ , whereas by using the small deformation tensor invariant it can be proven, see e.g. [10]

$$c_{55} = \frac{1}{2}(c_{22} - c_{23}) \tag{3.27}$$

Afterwards, taking

$$\boldsymbol{\sigma} = \begin{bmatrix} \sigma_1 \\ \sigma_2 \\ \sigma_3 \\ \sigma_4 \\ \sigma_5 \\ \sigma_6 \end{bmatrix} \text{ and } \boldsymbol{\varepsilon} = \begin{bmatrix} \varepsilon_1 \\ \varepsilon_2 \\ \varepsilon_3 \\ \varepsilon_4 \\ \varepsilon_5 \\ \varepsilon_6 \end{bmatrix}$$

the relationship "stress - strain" representing the matrix form of constitutive equations for the annulus fibrosis with respect to the local coordinate system (LCS) will be of the form

$$\sigma = \mathbf{C}\boldsymbol{\varepsilon} \tag{3.28}$$

where  $C_{[6x6]}$  is the compliance matrix

$$\mathbf{C} = [c_{ij}] = \begin{bmatrix} c_{11} & c_{12} & c_{12} & 0 & 0 & 0 \\ c_{12} & c_{22} & c_{23} & 0 & 0 & 0 \\ c_{12} & c_{23} & c_{22} & 0 & 0 & 0 \\ 0 & 0 & 0 & c_{44} & 0 & 0 \\ 0 & 0 & 0 & 0 & c_{55} & 0 \\ 0 & 0 & 0 & 0 & 0 & c_{44} \end{bmatrix}$$
(3.29)

with the 6 different coefficients:  $c_{11} = E_1(1 - v_{23}^2)$ ,  $c_{12} = E_2(v_{12} + v_{23}v_{12})$ ,  $c_{22} = E_2(1 - v_{12}^2)$ ,  $c_{23} = E_2(v_{23} + v_{12}^2)$ ,  $c_{44} = G_{12}D$ ,  $c_{55} = G_{23}D$ ,  $D = 1 - 2v_{12}^2v_{23} - 2v_{12}^2 - v_{23}^2$ , whereas the inverse "strain - stress" relation will read

$$\boldsymbol{\varepsilon} = \mathbf{S}\boldsymbol{\sigma} \tag{3.30}$$

The equation (3.28) expresses the Cauchy stress tensor components  $\sigma_j$  dependence on the deformations  $\varepsilon_i$ , (i = 1, 2, ...6). In terms of previous assumptions imposed in Chapter III.A while solving our problem, we start from the small deformations theory that provides, e.g. [17]

$$\varepsilon_{ij} = \frac{1}{2}(u_{i,j} + u_{j,i}), \quad (i, j = 1, 2, 3)$$
 (3.31)

**Table 1:** Angles between the coordinates in the "old" and "new" coordinate system and corresponding directional cosines defined in the lamella domain

	1	2	 3
-	+α	$\alpha + \frac{\pi}{2}$	$\frac{\pi}{2}$
Ī	cosα	-sinα	0
	$\frac{\pi}{2} - \alpha$	+α	$\frac{\pi}{2}$
2	sinα	cosα	0
	$\frac{\pi}{2}$	$\frac{\pi}{2}$	0
3	0	0	1

**Table 2:** Directional cosines notation between the "old" and "new" coordinate system defined in the lamella domain

1 2	
1 2	3
	$\overline{l_{3ar{1}}}$
	$l_{3\bar{2}}$
$\bar{3}$ $l_{1\bar{3}}$ $l_{2\bar{3}}$	$l_{3\bar{3}}$

where  $u_i$  are the displacement vector  $\mathbf{u}(X)$  components,  $X \in \Omega$  and  $u_{\bullet,i}$  means the derivation of the item  $u_{\bullet}$  with respect to  $x_i$ . The resulting matrix of elastic moduli, the compliance matrix  $\bar{\mathbf{s}}_{ij} = [\bar{s}_{ij}]$  with regarding to the GCS of the annulus fibrosis can be obtained from the relationship

$$\bar{\mathbf{s}} = \frac{1}{2}[(\bar{s}_{ij}(+\alpha) + \bar{s}_{ij}(-\alpha))], \quad (i, j = 1, 2, ..., 6)$$
 (3.32)

i.e the averaging of the elastic moduli due to annulus fibrosis being layered and to the orientation within the particular lamellae. By using the same procedure, the relationship for the elastic coefficients can be derived, where

$$\bar{\mathbf{c}} = \frac{1}{2} [(\bar{c}_{ij}(+\alpha) + \bar{c}_{ij}(-\alpha))], (i, j = 1, 2, ..., 6)$$
 (3.33)

# 3.4 Transformation of the elastic parameters when the system of coordinates is rotated

Let us consider a case where a "new" system  $(\bar{1}, \bar{2}, \bar{3})$  originates from the "old" one (1, 2, 3) by its rotation about 3 axis by the angle  $\alpha$ , see Fig. 2. Tab. 1 provides the relationships between the "old" and "new" coordinate system and corresponding directional cosines. The stress tensor components transformation from LCS to GCS reads, see e.g [14]

$$\bar{\boldsymbol{\sigma}} = \mathbf{L}\boldsymbol{\sigma}\mathbf{L}^T \tag{3.34}$$

where

$$\mathbf{L} = \begin{bmatrix} l_{1\bar{1}} & l_{2\bar{1}} & l_{3\bar{1}} \\ l_{1\bar{2}} & l_{2\bar{2}} & l_{3\bar{2}} \\ l_{1\bar{3}} & l_{2\bar{3}} & l_{3\bar{3}} \end{bmatrix}, \quad \bar{\boldsymbol{\sigma}} = [\bar{\sigma}_{ij}], (i, j = 1, 2, 3) \quad (3.35)$$

is the transformation matrix. Moreover, the backward transformation (from GCS to LCS) reads

$$\boldsymbol{\sigma} = \mathbf{L}^T \bar{\boldsymbol{\sigma}} \mathbf{L} \tag{3.36}$$

Both (3.34) and (3.36) can be rewritten in tensor inscription

$$\bar{\sigma}_{kl} = \sigma_{ij} l_{ki} l_{lj}, \quad (i, j = 1, 2, 3), (k, l = 1, 2, 3)$$
 (3.37)

and

$$\sigma_{ij} = \bar{\sigma}_{kl} l_{ki} l_{li}, \quad (i, j = 1, 2, 3), (k, l = 1, 2, 3)$$
 (3.38)

In the process of the elastic constants transformation relations deriving we start from elastic potential expression with regard to the GCS and to the LCS, that are equal from the physical point of view. We know that

$$W(\varepsilon_{ij}) = W(\bar{\varepsilon}_{ij}), \quad (i = 1, 2..., 6)$$
 (3.39)

$$W(\sigma_{ij}) = W(\bar{\sigma}_{ij}), \quad (i = 1, 2..., 6)$$
 (3.40)

In the following, the deriving of (3.40) is shown. When writing this equation in detail we get

$$\begin{split} \frac{1}{2}c_{11}\varepsilon_{1}^{2} + c_{12}\varepsilon_{1}\varepsilon_{2} + \ldots + \frac{1}{2}c_{66}\varepsilon_{6}^{2} &= \frac{1}{2}\bar{c}_{11}\bar{\varepsilon}_{1}^{2} + \bar{c}_{12}\bar{\varepsilon}_{1}\bar{\varepsilon}_{2} + \ldots \\ &+ \frac{1}{2}\bar{c}_{66}\bar{\varepsilon}_{6}^{2} \end{split} \tag{3.41}$$

Substituting  $\varepsilon_i$  as functions of parameters  $(\bar{\varepsilon}_1, ... \bar{\varepsilon}_6)$  for (i = 1, 2, ..., 6) and applying for the deformation tensor components, (3.5), and comparing the coefficients next to the deformation components  $\varepsilon_i$  squared and products  $\bar{\varepsilon}_i\bar{\varepsilon}_i$ we obtain the relationship between elastic coefficients  $c_{ii}$ and  $\bar{c}_{ii}$ . The coefficients  $\bar{c}_{ii}$  stand as linear functions of  $c_{ii}$ , being homogeneous functions of the 4-th degree with regard to  $l_{i\bar{i}}$ . The complicated expressions that arise can be shortened by establishing the additional parameters  $q_{ij}$ , see Tab. 3 and Tab. 4, where e.g.  $q_{11} = l_{1\bar{1}}^2$ ,  $q_{43} = 2l_{2\bar{3}}l_{3\bar{3}}$ , etc. by using the parameters q we can express the transformation relations in the form

$$\bar{s}_{ij} = s_{mn} q_{im} q_{in} \tag{3.42}$$

$$\bar{c}_{ij} = c_{mn}q_{im}q_{jn} \tag{3.43}$$

Another method of elastic coefficients and elastic moduli transformation while switching between two different coordinate systems is performed by [5].

$$\bar{c}_{ijkl} = l_{im}l_{jn}l_{ko}l_{lp}c_{mnop}$$
  $\bar{s}_{ijkl} = l_{im}l_{jn}l_{ko}l_{lp}s_{mnop}$  (3.44)

that represents two systems of 81 equations with 81 unknowns. Due to symmetry, that number can be decreased to 21.

# 4 Numerical analysis and computation

After discretization and approximation due to finite analysis analysis, the total potential energy functional involved in Lagrange variational principle, see (3.4), can be expressed as follows:

$$\boldsymbol{\Pi} = \frac{1}{2} \mathbf{u}^T \mathbf{K} \mathbf{u} - \mathbf{u}^T \mathbf{f} \tag{4.1}$$

where  $\mathbf{K} = \mathbf{B}^T \mathbf{C} \mathbf{B}$  is the stiffness matrix  $\mathbf{B}$  being physical and C geometrical matrix of the discretized system and  $\mathbf{f} = \mathbf{f}_h + \mathbf{f}_t$  is the nodal force vector, the sum of volume body force and force due to the traction.

Let us recall that the resulting system of linear equations  $\mathbf{K}\mathbf{u} = \mathbf{f}$  involves the axisymmetry in case of anisotropy.

Finally, the following the boundary conditions accomplish the mathematical model:

$$u_z(r, t, z) = 0$$
 for  $z = 0$  (4.2)

$$u_r(r, t, z) = 0$$
 for  $r = 0$  (4.3)

$$u_r(r, t, z) = 0$$
 for  $r = 0$  (4.3)  
 $p = \frac{P}{A}$  for  $z = H$  (4.4)

with H being the height of the disc, see Fig. 1, P the traction and A the area magnitude of upper endplate; endplates are the tissue plate covering the entire disc one at its top and its bottom. It is the thin tissue member that attaches the disc and the vertebra. Within the software based on the finite element method, the elements LINK8 (spar 2nodes 3D element) and SOLID185 (brick 8 node 3D element) with linear approximating function were used.

# 4.1 Example of biomechanical computation

Numerical treatment and computation is based on the finite element method. The derived relations and acquired knowledge together with the finite element tool are utilized for the stress and strain analysis of the treated twophased ambient. The object of our investigation is the intervertebral disc ID 2/3, the one between the second and the third human lumbar vertebrae and its annulus fibrosis. The anatomy of the disc can be seen e.g. in [13]. We compute the mechanical response of the domain due to external axial load.

Intervertebral disc geometry

We take the dimensions of the intervertebral disc from [12]. The disc height is H = 1.2 cm, upper and lower endplate area 22 cm<sup>2</sup>, or equivalent outer circular radius  $r_0$  = 2.64 cm. The measurement of [12]

**Table 3:** Additional parameters  $q_{ii}$ 

j	1	2	3	4	5	6
1	$l_{1\bar{1}}^2$	$l_{1\bar{2}}^2$	$l_{1\bar{3}}^{2}$	$l_{1\bar{2}}l_{1\bar{3}}$	$l_{1\bar{3}}l_{1\bar{1}}$	$l_{1\bar{2}}l_{1\bar{1}}$
2	$l_{2\bar{1}}^2$	$l^2_{2\bar{2}}$	$l^2_{2\bar{3}}$	$l_{2\bar{2}}l_{2\bar{3}}$	$l_{2\bar{3}}l_{2\bar{1}}$	$l_{2\bar{2}}l_{2\bar{1}}$
3	$l_{3\bar{1}}^2$	$l^2_{3ar{2}}$	$l^2_{3\bar{3}}$	$l_{3\bar{2}}l_{3\bar{3}}$	$l_{3\bar{3}}l_{3\bar{1}}$	$l_{3\bar{2}}l_{3\bar{1}}$
4	$2l_{3\bar{1}}l_{2\bar{1}}$	$2l_{3\bar{2}}l_{2\bar{2}}$	$2l_{3\bar{3}}l_{2\bar{3}}$	$l_{3\bar{3}}l_{2\bar{2}}+l_{3\bar{2}}l_{2\bar{3}}$	$l_{3\bar{3}}l_{2\bar{1}}+l_{3\bar{1}}l_{2\bar{3}}$	$l_{3\bar{1}}l_{2\bar{2}}+l_{3\bar{2}}l_{2\bar{1}}$
5	$2l_{3\bar{1}}l_{1\bar{1}}$	$2l_{3\bar{2}}l_{1\bar{2}}$	$2l_{3\bar{3}}l_{1\bar{3}}$	$l_{3\bar{3}}l_{1\bar{2}}+l_{3\bar{2}}l_{1\bar{3}}$	$l_{3\bar{3}}l_{1\bar{1}}+l_{3\bar{1}}l_{1\bar{3}}$	$l_{3\bar{1}}l_{2\bar{2}}+l_{3\bar{2}}l_{1\bar{1}}$
6	$2l_{2\bar{1}}l_{1\bar{1}}$	$2l_{1\bar{2}}l_{2\bar{2}}$	$2l_{1\bar{3}}l_{2\bar{3}}$	$l_{1\bar{3}}l_{2\bar{2}}+l_{1\bar{2}}l_{2\bar{3}}$	$l_{1\bar{3}}l_{2\bar{1}}+l_{1\bar{1}}l_{2\bar{3}}$	$l_{1\bar{1}}l_{2\bar{2}}+l_{1\bar{2}}l_{2\bar{1}}$

**Table 4:** Goniometrical transcription of the parameters  $q_{ij}$  with  $c=cos\alpha$  and  $s=:sin\alpha$ 

j	1	2	3	4	5	6
1	$c^2$	$s^2$	0	0	0	CS
2	$s^2$	$c^2$	0	0	0	-cs
3	0	0	1	0	0	0
4	0	0	0	С	-s	0
5	0	0	0	S	C	0
6	-2cs	2cs	0	0	0	$c^2-s^2$

reveals that nucleus pulposus occupies 20 - 50% of the disc axial cross section area, accordingly we take the inner radius  $r_I = 0$ ,  $707r_O$ .

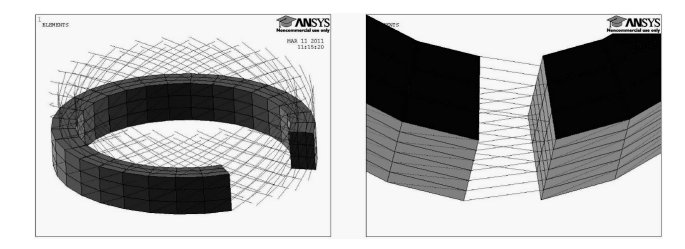
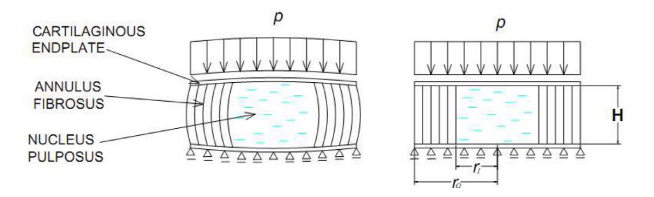


Figure 3: Fibres configuration in the amorphic base substance within the annulus fibrosis finite element model

### - Physical characteristics of the materials

- Annulus fibrosis is modelled as a transversally isotropic body, i.e. a system of thin concentric cylindric shells of constant thickness. The fibres material characteristics are taken as acquired from experimental measurements [4]:  $E_1 = 334$  MPa,  $E_2 = 9.5$  MPa,  $V_{12} = 0.5$ ,  $V_{23} = 0.05$ ,  $G_{12} = 1.9$  MPa,  $G_{23} = 4.523$  MPa. These properties was incorporated in **C** matrix in (3.30) and used afterwards in the computation within the FEM software.



**Figure 4:** Anatomical (left) and simplified (right) representation of a human intervertebral disc - axial section. Applied distributed load is represented by uniform arrows above.

- Cartilaginous endplate region is regarded as an isotopic homogeneous material of the thickness 0.06 cm with a modulus 24.3 MPa and Poisson ratio 0.45 [18].
- Nucleus pulposus (NP) is modelled as an incompressible liquid. It is enclosed by the annulus fibrosis from the side and endplates from the top and bottom. Water content in NP decreases with the age from the natal value of 88% to 69% at the age of 79 [16]. For our computing the values of 0.49 for the Poisson ratio and 0.013 MPa for Young elastic modulus were taken.

#### - Load

We carried out the computation on the human intervertebral disc with the load P = 450 N which acts at the endplate of the disc L2/L3, i.e. the corresponding uniformly distributed load p[Pa], is taken p = P/A with  $A = \pi r_0^2$  [8].

#### Results

Fig. 5 and Fig. 6 provide the graphical information about the disc deformation under the load.

The graphs in Fig. 8–10 interpret the comparison of the two approaches. The comparison of displacement, strain and stress values are performed on the outside meridian line. Herein, the "Path", i.e. the bottom-to-up oriented vertical meridian line stands

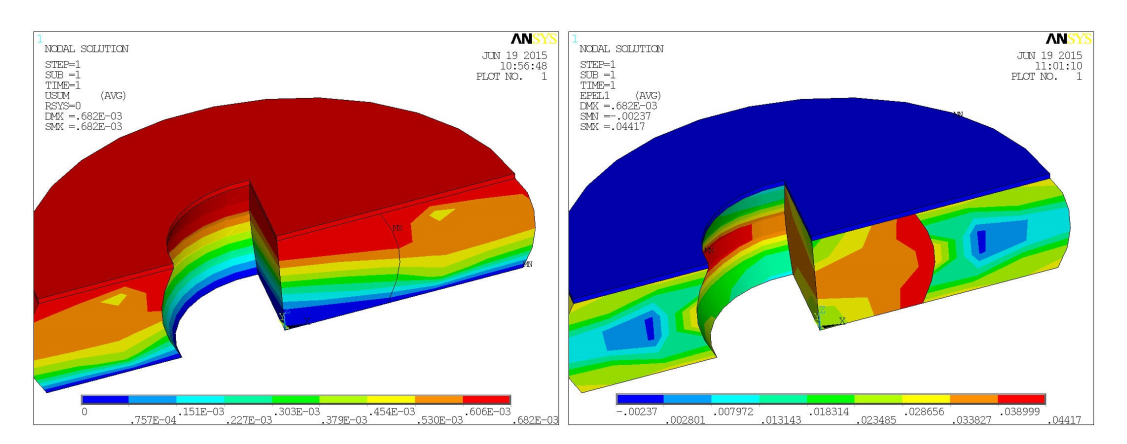


Figure 5: The ID mechanical behaviour with anisotropy homogenization approach used; displacement isolines (upper), strain isolines (lower)

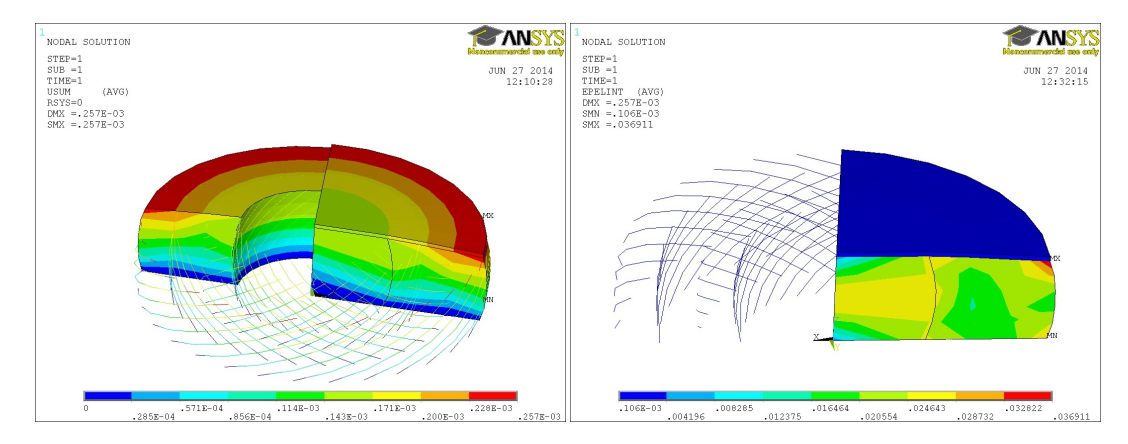
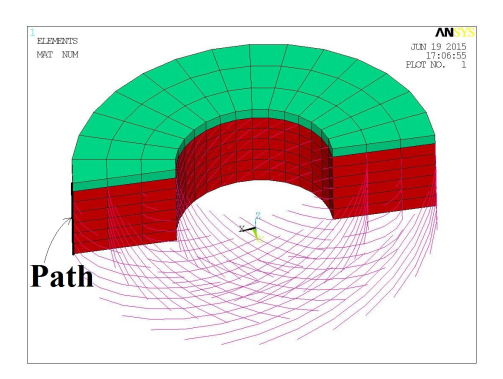


Figure 6: The results - displacement (upper picture), strain values (lower picture) obtained on the intervertebral disc model with complex geometry approach where particular fibres geometry were developed within the software



**Figure 7:** AF with Path highlighted that stands as an abscissa in the comparison graphs. Along Path the results are observed an the comparison is carried out.

the abscissa of these three graphs, see Fig. 7. Corresponding numerical value can be seen in Table 5.

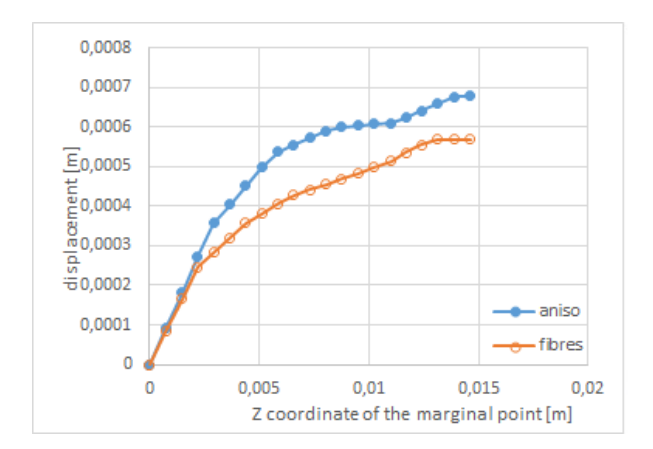
## 4.2 Discussion

As the disc is exposed to the vertical pressure acting on the upper surface, as a whole it is stretched laterally and squeezed vertically. At the same time the soft annulus fibrosis deforms aside enabling incompressible nucleus to keep its volume unchanged. It is apparent from the Fig.5 and Fig.6 that the strain is greater in nucleus pulposus than in annulus fibrosis. As the endplate is significantly stiffer, its strain remains very small.

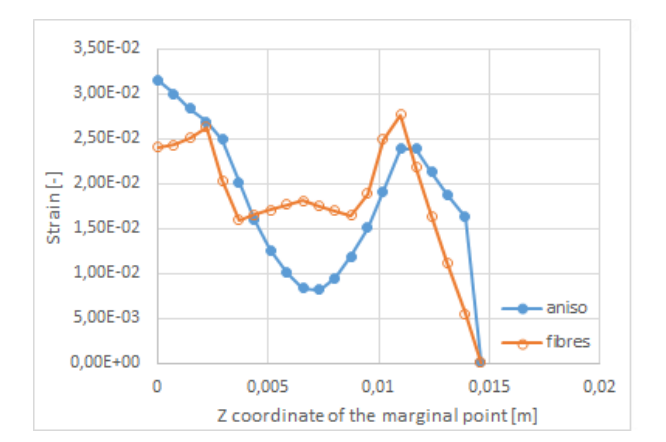
As the comparison of both approaches was done on the intervertebral disc with upper and without bottom endplate, see e.g. Fig. 7, the tissue is soft from the very bottom up to the endplate altitude. That is why the magnitude of the von Mises stress is very small along this part of the "Path". When proceeding upward along the soft tissue (still on the Path), the stress still remains of a small magnitude until approaching to the stiffer endplate, when the magnitude of the stress increase rapidly, see Fig. 10.

Table 5: Displacement, strain and von Mises stress values along the Path

	Displacement		Von Mis	es Strain	Von Mises stress	
Z coor	anizo	fibres	anizo	fibres	anizo	fibres
0	0	0	3,16E-02	2,41E-02	-6,91E-02	4,88E+05
7,30E-04	9,09E-05	8,27E-05	3,00E-02	2,43E-02	0,20281	4,87E+05
1,46E-03	1,82E-04	1,65E-04	2,84E-02	2,51E-02	0,62332	4,96E+05
2,19E-03	2,73E-04	2,45E-04	2,69E-02	2,63E-02	1,0624	5,08E+05
2,92E-03	3,57E-04	2,83E-04	2,49E-02	2,04E-02	1,3615	4,47E+05
3,65E-03	4,04E-04	3,21E-04	2,02E-02	1,60E-02	0,92354	3,92E+05
4,38E-03	4,52E-04	3,57E-04	1,60E-02	1,66E-02	0,53526	3,49E+05
5,11E-03	4,99E-04	3,81E-04	1,26E-02	1,71E-02	0,75871	3,38E+05
5,84E-03	5,37E-04	4,06E-04	1,01E-02	1,77E-02	0,93663	3,31E+05
6,57E-03	5,55E-04	4,28E-04	8,39E-03	1,81E-02	0,93425	3,29E+05
7,30E-03	5,73E-04	4,41E-04	8,21E-03	1,75E-02	0,93305	3,37E+05
8,03E-03	5,91E-04	4,55E-04	9,55E-03	1,70E-02	0,93317	3,49E+05
8,76E-03	6,01E-04	4,68E-04	1,19E-02	1,65E-02	0,80453	3,74E+05
9,49E-03	6,04E-04	4,83E-04	1,51E-02	1,89E-02	0,87604	4,32E+05
1,02E-02	6,07E-04	4,98E-04	1,92E-02	2,49E-02	1,2568	4,98E+05
1,10E-02	6,10E-04	5,14E-04	2,39E-02	2,77E-02	1,6414	6,30E+05
1,17E-02	6,23E-04	5,35E-04	2,39E-02	2,18E-02	1,71E+05	9,61E+05
1,24E-02	6,41E-04	5,55E-04	2,13E-02	1,64E-02	4,32E+05	1,32E+06
1,31E-02	6,58E-04	5,69E-04	1,88E-02	1,12E-02	6,92E+05	1,32E+06
1,39E-02	6,76E-04	5,69E-04	1,63E-02	5,56E-03	9,53E+05	1,20E+06
1,46E-02	6,79E-04	5,69E-04	1,88E-04	9,63E-05	2,34E+06	1,91E+06



**Figure 8:** Displacement values comparison along the Path yielded by the two approaches; "aniso" - our approach developed in the paper, "fibres" - the approach with the complex geometry



**Figure 9:** Stress values comparison along the Path yielded by the two approaches; "aniso" - our approach developed in the paper, "fibres" - the approach with the complex geometry

# 5 Conclusion

The main contribution of the investigation described in the paper is the derivation of the anisotropic material tensor within the approach named "aniso". It represents the complex geometry and involves the material properties of all components, as well. The number of 21 material characteristics needed in the complex geometry model called "fibres" decreased to 6 in "aniso". The anisotropic tensor built up incomes afterwards to the finite element model that computes the mechanical response of the intervertebral disc to the mechanical load. The presented results reveal the feasibility of the approach developed. Within the computation both approaches are compared: "Aniso"

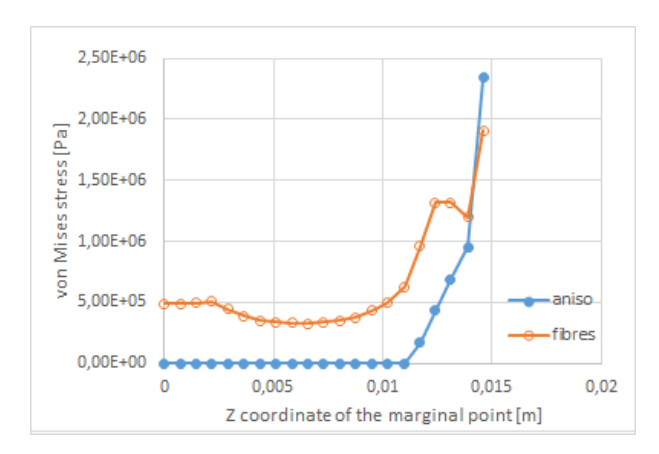


Figure 10: Strain values comparison along the Path yielded by the two approaches; "aniso" - our approach developed in the paper, "fibres" - the approach with the complex geometry

where the developed material tensor of anisotropy is used (6 physical constants), and "fibres" with the complex geometry of the annulus fibrosis used, with individual fibres and 21 their particular material properties given. As the results of both computations match very well, it is apparent that our approach is feasible and it facilitates the computation significantly. The approach is applicable to a uniform tension load as well (e.g. load during sport or rehabilitation exercises).

The future work will be focused on the combined load, as an eccentric loading and torsion. Moreover, as the nucleus pulposus physical properties change with the age of its holder, it will be worth to involve time dependence into the model.

**Acknowledgement:** The authors acknowledge the financial support of grant APVV 0184-10.

# References

- Anderson D.G., Risbud M.V., Shapiro I.M., Vaccaro A.R., Albert T.J., Cell-based therapy for disc repair, Spine J., 2005, 5, 297-303
- [2] Belytschko T., Kulak R., Schultz A., Galante J., Finite element stress analysis of an intervertebral disc, J. Biomechanis, 1974, 7, 277-285
- [3] Chao E.S., Simulation technology for biomechanical analysisof the muscoskeletal system, Acta of Bioengineering and Biomechanis, 2002, 4, 23-29
- [4] Galante J.O., Tensile properties of the human lumbar annulus fibrosis, Acta Ortop. Scand., 1967
- [5] Hearmon R.F.S., Introduction to applied anisotropic elasticity, The Clarendon Press. Oxford 1961
- [6] Cheney W., Kincaid D., Numerical Mathematics and Computing, Thomsom Learning, 2004

- [7] Kisel'ák J., Pardasani K., Adlakha N., Stehlík M., Agrawal M., On Some Probabilistic Aspects of Diffusion Models for Tissue Growth, Open Statistics and Probability Journal, 2013, 5, 14-21
- [8] Konvičková S., Valenta J., Biomechanics of human muscoskeletal system II, Publ. House ČVUT Prague, 2007, (in Czech)
- [9] Kulak R., Belytchko T., Schultz A., Galante J., Nonlinear behavior of the human intervertebral disc under axial load, J. Biomechanis. 1976. 8, 377-386
- [10] Lechnickij S.G., Theory of elasticity of the anisotropic body, Gostechizdat, 1957, (in Russian)
- [11] Michlin S.G., Variational methods in mathematical physics, Nauka, 1970, (in Russian)
- [12] Rolander S.D., Motion of the lumbar spine with special reference to the stabilizing effect of posterior fusion, PhD Thesis, American Transactions of Engineering and Applied Sciences, 2012
- [13] Sinelnikov R.D., Human anatomy atlas, Avicenum, 1982, (in Czech)
- [14] Sokolnikoff J.S., Mathematical theory of elasticity, MacGraw-Hill, 1950
- [15] Spilker R.L., A Sipmlified Hybrid-stress Finite Element Model of the Intervertebral Disc, Conference Proceedings, Finite Element in Biomechanics, Tuscon, Arizona, 1982, 295-312
- [16] Valenta J., et al., Biomechanics, Academia, Prague, 1985, (In Czech)
- [17] Washitzu K., Variational methods in elasticity and plasticity, Pergamon Press. 1982
- [18] Yamada H., Strength of biological material, Williams & Wilkins edition, 1972